J Nanostruct 16(3): 3270-3279, Summer 2026

RESEARCH PAPER

Influence of Chromium Incorporation on the Structural, Optical, and Magnetic Behaviour of Cu_2ZnSnS_4 Nanomaterial

Sara K. Naif

Department of Dairy Science and Technology, College of food science, Al-Qasim Green University, Iraq

ARTICLE INFO

Article History:
Received 02 April 2026
Accepted 16 May 2026
Published 01 July 2026

Keywords:
Chromium Doping
Magnetic Properties
Nanostructured Materials
Optical Properties
Structural Properties

ABSTRACT

The $Cu_2Zn_{1-x}Cr_xSnS_4$ (x=0- 1) compound was synthesized by sol-gel method in order to modulate the structural and morphological characteristics of the compound. XRD studies revealed that there is small variation of lattice constants with slight distortion in crystal structure due to partial substitution (Cr) which confirms the successful entrance of Cr^{2+} ions into the Cu_2ZnSnS_4 lattice. While Raman confirmed the formation of a pure Cu_2ZnSnS_4 phase with slight peak shifting due to the substitution, FESEM images demonstrated that the particle size ranged in the nanoscale with a regular surface distribution. Photoluminescence measurements indicate that increasing chromium content causes changes in the optical bandgap, potentially leading to modifications in the optical properties. Meanwhile, magnetic analysis confirms that increasing chromium content directly affects the magnetic properties of the compound, causing it to shift from paramagnetic to weakly magnetic behaviour. The results show that the optical and magnetic properties of the Cu_2ZnSnS_4 compound can be changed by replacing zinc with chromium, which enhances its use in photocatalysis and thin-film solar cells.

How to cite this article
Naif S. Influence of Chromium Incorporation on the Structural, Optical, and Magnetic Behaviour of Cu_2ZnSnS_4 Nanomaterial. J Nanostruct, 2026; 16(3):3270-3279. DOI: 10.22052/JNS.2026.03.022

INTRODUCTION

Recently, thin-film solar cells have become one of the most promising renewable energy technologies due to their economic efficiency and environmental friendliness. The compound Cu_2ZnSnS_4 (CZTS) is used as a light-absorbing thin film due to its excellent photoelectric properties, plentiful and non-toxic elements, and suitable atomic structure [1.2]. Studies indicate that the optical and magnetic properties of the CZTS make it a possible alternative to traditional solar materials such as $CuInGaSe_2$ and CdTe [3.4]. This compound has a tetragonal crystal structure of the kesterite type and has a straight energy band gap ranging between 1.4 and 1.5 eV, making it suitable for light absorption in the visible spectrum [5.6]. One recent trend in improving CZTS performance is chromium (Cr) doping. Studies have shown that adding chromium to CZTS can lead to the formation of an intermediate band within the energy bandgap, allowing for additional light absorption and improving solar cell efficiency [7]. In addition, it is believed that chromium doping can improve the magnetic properties of the compound, opening new prospects for intermediate-band solar cell applications

* *Corresponding Author Email: sarra@fosci.uoqasim.edu.iq*

[8-10]. Regardless of the great ability of the chromium-doped CZTS, there are challenges with crystal stability and structural symmetry. These challenges require research and development to improve the overall properties and ensure the stability of practical applications. This manuscript focuses on the effects of chromium doping on structural, optical and magnetic properties of $Cu_2Zn_{1-x}Cr_xSnS_4$ (x = 0-1), which has not been detected much in previous studies. While most previous studies have focused on replacing certain elements to improve photovoltaic properties of traditional CZTS compounds or increase the solar performance, this manuscript presents an integrated study that adds structural analysis, optical and magnetic characterization in a single context, playing effective role in the distribution of nanoparticle distribution. The use of novel preparation methods and controlled doping ratios provides a new scientific basis for understanding the structure-application relationship, opening up prospects for the design of innovative CZTS materials applicable to photocatalysis and thin-film solar cells, and laying the foundation for the development of nanomaterials with precisely optimized multiple properties.

MATERIALS AND METHODS

Preparation method and Characterization

$Cu_2Zn_{1-x}Cr_xSnS_4$ at (x=0-1) was prepared using the sol-gel method using chlorides as primary metal precursors. Copper(II) chloride $CuCl_2$ $2H_2O$, zinc chloride $ZnCl_2$, chromium(II) chloride $CrCl_2$ (with substitution ratios x = 0.0, 0.25, 0.5, 0.75, 1), tin(II) chloride $SnCl_2$ $2H_2O$, and thiourea (CH_4N_2S) were used as the sulfur source. The salts were dissolved in 100 ml of distilled ethanol at initial concentrations ranging from 0.1–0.2 mol/L, maintaining the general molar ratio of the metals according to the formula Cu: (Zn+Cr): Sn: S = 2:1:1:4. To ensure better homogeneity and prevent premature precipitation, citric acid ($C_6H_8O_7$) was added at a molar ratio approximately 1.5 times the total amount of metal cations as a complexing agent, with ethylene glycol ($C_2H_6O_2$) added at a volume ratio (10–15 mL) as a copolymer to form a cohesive gel network. The mixture was then continuously stirred using a magnetic stirrer at 75–80 °C for 3 h until a clear, homogeneous solution was obtained. The solution was allowed to gradually thicken to form a homogeneous gel, and the resulting gel was then dried in an oven at 110°C for 12 h to obtain a solid gel. Subsequently, the gel was preheated at 300°C for 2 h to remove organic residues and thermally decompose intermediates. Finally, it was annealed at 500°C for 2 h in an inert argon (Ar) atmosphere with an excess of sulfur from the decomposition of thiourea to ensure the formation of a pure kesterite-type crystalline phase of $Cu_2Zn_{1-x}Cr_xSnS_4$. The final product was a homogeneous dark brown Nano-powder, which was used for structural (XRD, Raman), morphological (FESEM), optical (UV–Vis, PL), and magnetic (VSM) investigations to evaluate the effect of partial and total chromium substitution on the properties of the compound.

RESULTS AND DISCUSSION

Crystal structure properties

As shown in the Fig. 1, XRD patterns of $Cu_2Zn_{1-x}Cr_xSnS_4$ (x = 0 → 1) samples showed characteristic peaks consistent with the tetragonal kesterite phase, with the dominant peak associated with the (112) plane located at 2θ about 28.40°, as typical for pure CZTS. As summarized in Table 1, the position of the dominant peak shifts towards lower angles accompanied by a slight decrease in d-spacing, indicating a local distortion in the unit cell and a change in bond size due to ionic substitution [11,12]. In addition, it is noted that the lattice constants “a” and “c” have gradually decreased, which has led to a decrease in the unit cell volume (V) to its lowest value. Computational and experimental studies indicate that ionic substitutions may change the distance between layers and lead to local expansion or contraction depending on the oxidation state and spatial symmetry [12,13].

From a nanocrystalline perspective, peak width data and Scherer calculations show that crystallite size was decreased accompanied by an increase in the microstrain. This trend (decreasing crystallite size with increasing microstrain) is consistent with the interpretation that partial Cr substitution generates localized defects and distortions that broaden the crystal size distribution and lead to broadening of the XRD peaks (i.e., increased peak width); that may reflect the formation of a larger secondary phase or crystallographic rearrangement that reduces the lattice distortions seen in the intermediate-strain samples. The interpretation of shifts in magnitude and reflection is consistent with Scherer’s concepts and analysis of peak amplitude [14,15]. The transient decrease

in the lattice constants and unit cell volume with increasing internal stress could be due to the introduction of a Cr ion with a different oxidation/coordination state that produces a different binding energy and tends to induce local tension (e.g., Cr^{2+} or Cr^{3+} at tetrahedral/ other sites) compared to Zn^{2+}, thus showing a localized increase in d-spacing. The subsequent decrease in crystallite size and the increase in the microstrain correspond either to a better lattice rearrangement upon complete substitution or to the emergence of phase separation that produces

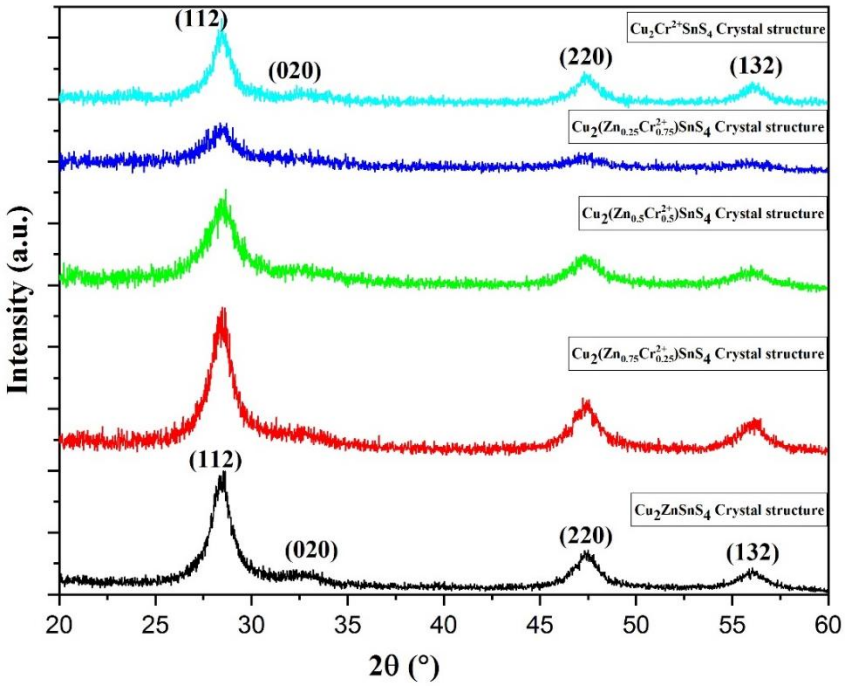

Fig. 1. XRD pattern of the $Cu_2Zn_{1-x}Cr_xSnS_4$ compound at (x = 0–1).

Table 1. Crystal structure parameters of $Cu_2Zn_{1-x}Cr_xSnS_4$ doped Cr^{2+} compounds at (x=0, 0.25, 0.5, 0.75, 1).

Compounds	x = 0	x= 0.25	x = 0.5	x = 0.75	x = 1
Diffraction dominant peak 2θ (°)	28.3929	28.3962	28.4030	28.4034	28.4021
Lattice constants "*a*, *c*" (Å)	*a* = 5.4261 *c* = 10.937	*a* = 5.4233 *c* = 10.934	*a* = 5.4247 *c* = 10.936	*a* = 5.4259 *c* = 10.932	*a* = 5.4249 *c* = 10.935
c/a	2.0156	2.0161	2.0159	2.0147	2.0157
$V=a^2c$ (Å^3)	322.013	321.5928	321.8177	321.842	321.812
η=c/2a	1.0078	1.0081	1.0079	1.0074	1.0078
Crystallite Size only (nm)	5.577	5.572	5.548	5.432	5.516
Micro Strain (%)	0.02534	0.02748	0.03743	0.03981	0.02489

larger coherent domains of a different phase [16]. Previous studies on addition/substitution effects in CZTS indicate a deterioration in crystallinity or the emergence of secondary phases upon certain Cr additions, which supports caution in interpreting the increase in crystallite size as a pure function of the quality of a single phase [17]. Therefore, it can be said that the XRD results of $Cu_2Zn_{1-x}Cr_xSnS_4$ indicate that all samples retain the kesterite crystal structure with slight shifts in peak positions

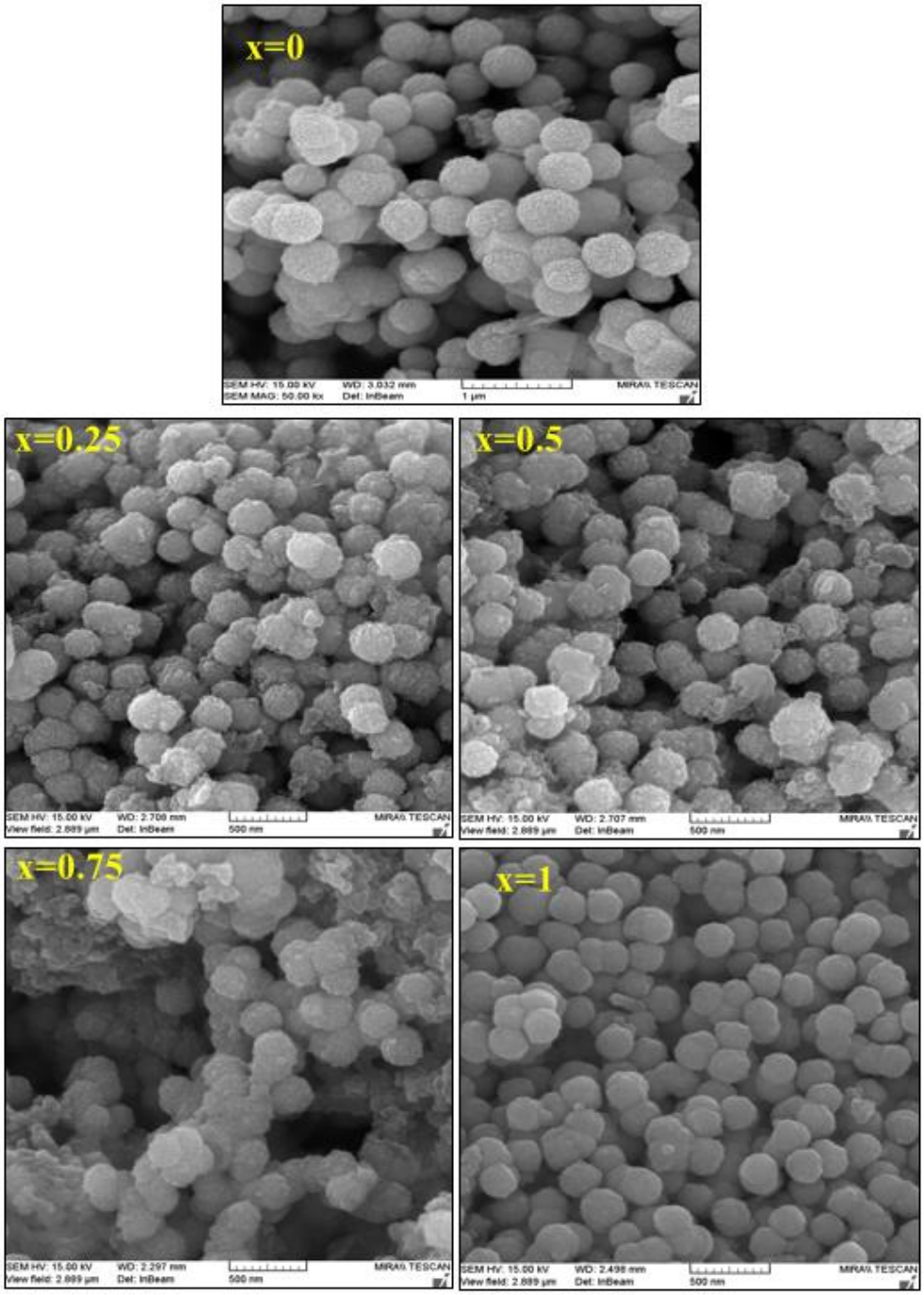

Fig. 2. Morphology of nanoparticles of the $Cu_2Zn_{1-x}Cr_xSnS_4$ compound at (x = 0–1).

and significant changes in the lattice constants and unit cell volume due to the gradual replacement of Zn by Cr. They also indicate a temporary decrease in the unit cell volume and increase micro-stress at medium substitution ratios accompanied by a decrease in crystallite size, indicating the generation of local lattice distortions.

Morphological analysis

Scanning electron microscope (FESEM) images of the $Cu_2Zn_{1-x}Cr_xSnS_4$ compound at (x = 0–1) show that the particles have a quasi-spherical morphology with varying degrees of compactness and agglomeration. The grain size varies with the substitution ratio. In pure (x = 0), the particles seem relatively large with a rough, inhomogeneous surface, while in the intermediate ratio (x = 0.25 and x = 0.5), the particles become smaller and more homogeneous, compatible in the form of investigation and increase in microstrain in the XRD results. At x = 0.75, the high lattice stress resulted in a more porous structure with irregular agglomerates. Conversely, at x = 1, the structure became more uniform and the grain distribution more homogeneous due to increased crystal size and reduced internal stress. The particle size, distribution, and shape of nanoparticles play a crucial role in studying the optical properties of nanomaterials such as light absorption and PL emission spectrums. Studies have shown that smaller, more homogeneous nanoparticles exhibit higher absorption intensity, and the pores and surface aggregates improve light scattering within the layer and reduce light reflection, thus improving light absorption efficiency in photovoltaic or catalytic applications [18-20]. Therefore, as shown in Fig. 2, particles with a precise and uniform spherical shape may be suitable for improving light absorption and scattering due to their compact structure and uniform particle size distribution. Particles exhibiting irregular or porous aggregates may improve absorbance, but with the potential for increased undesirable scattering. A uniform structure at x = 1 provides a balance between scattering and light absorption, making these samples candidates for balanced optical performance.

Optical properties

It is noted from the Figs. 3 and 4 that the $Cu_2Zn_{1-x}Cr_xSnS_4$ compound exhibits a slight variation in the energy gap between samples. This small variation is consistent with the effects of crystal size and surface distortions and defects associated with the nanoscale morphology. Decreasing crystallite size and increasing microstrain typically lead to broadened Urbach tails and small shifts in the absorption edge, while improved homogeneity and larger grains tend to reduce these spectral extensions [21,22]. A sample with a homogeneous, spherical, and moderately packed appearance exhibits greater overall absorption, possibly due to a combination of increased effective surface area for absorption and enhanced internal light scattering/diffusion within the aggregated particles. Samples with porous/non-uniform agglomerations (e.g., x≈0.75) may exhibit different absorption behavior due to a conflicting balance between increased surface area and increased scattering losses, as the morphology and particle distribution affect the absorption extension and line-edge efficiency [23,24].

The change in energy gap values may be attributed to a slight change in chemical composition/ionic substitution (difference between Zn and Cr) which changes the structure of the electron bands, a change in crystallite size as well as the effect of defects and band tails/ Urbach which increases the absorption below the edge. As shown in Fig. 5, the fluorescence spectrum (PL) is shown in different distinct peaks (380–420 nm) located in the violet-blue area, indicating electronic transitions associated with energy levels near the band gap. The peak position was observed to replace chromium-substituting conditions, to 383.85 nm from x = 0 to high values such as 418.45 nm at x = 0.25, and to settle at 414.43 nm at full replacement (x = 1). This change in peak positions reflects the effect of ionic replacement on the electronic structure, as it leads to revision of the energy level and redistribution of defect states within the optical gap [25]. In addition, the photoluminescence spectra show a marked variation in mid-peak width, ranging from 59.71 nm to 118.19 nm, possibly indicating the presence of numerous emission centers and a variety of defects, such as cation void defects V_{Cu} and V_{Zn} or localized defects [26]. The violet-blue emission is mainly attributed to radiation transfer between donor levels due to copper voids and acceptor levels, which are often associated with partial chromium substitution or crystal defects. The sample with x = 0.5, in particular, exhibited the lowest mid-peak width (76.71 nm), indicating

better crystalline structure regularity and fewer emission centers, thus improving emission efficiency [27]. Therefore, it can be argued that the optical properties of Cu_2ZnSnS_4 can be tuned by substituting zinc for chromium, i.e., by controlling the emission peak positions and breakpoints, making it suitable for photocatalysis and thin-film solar cell applications.

Raman Analysis

In order to study the formation of secondary phases in the compound $Cu_2(Zn_{1-x}Cr_x)SnS_4$ as a result of ionic substitution, Raman spectroscopy was used as shown in the Fig. 6. The positions of the main peaks are identified, their amplitudes are measured, the A symmetry and any additional peaks that may arise from secondary phases or crystal defects are distinguished, and the implications of the transitions in these peaks for crystal structure, nanoscale dimensions, and chemical composition are discussed Fig. 6a shows the Raman spectra of $Cu_2(Zn_{1-x}Cr_x)SnS_4$ at different chromium concentrations. The main peaks appear in the range (310-330 cm^{-1}), which is the characteristic vibrational range of the kesterite phase [28,29]. It is noted from Fig. 6b that the position of the main peak gradually shifts from 326 cm^{-1} in the pure sample (x = 0) to 309 cm^{-1} upon complete substitution (x = 1). This change to the lower values in the Raman shift reflects the effect of ionic replacement of Zn^{2+} with Cr^{2+} ions with small ionic radii, leading to a change in partial reorganization of the power and structure of the vibration bonds in the crystal grid [30]. Raman confirms the stable crystalline structure of the spectrum connection and fits what was seen in the XRD pattern. The intensity and positions of the peaks also indicate that the basic compensation

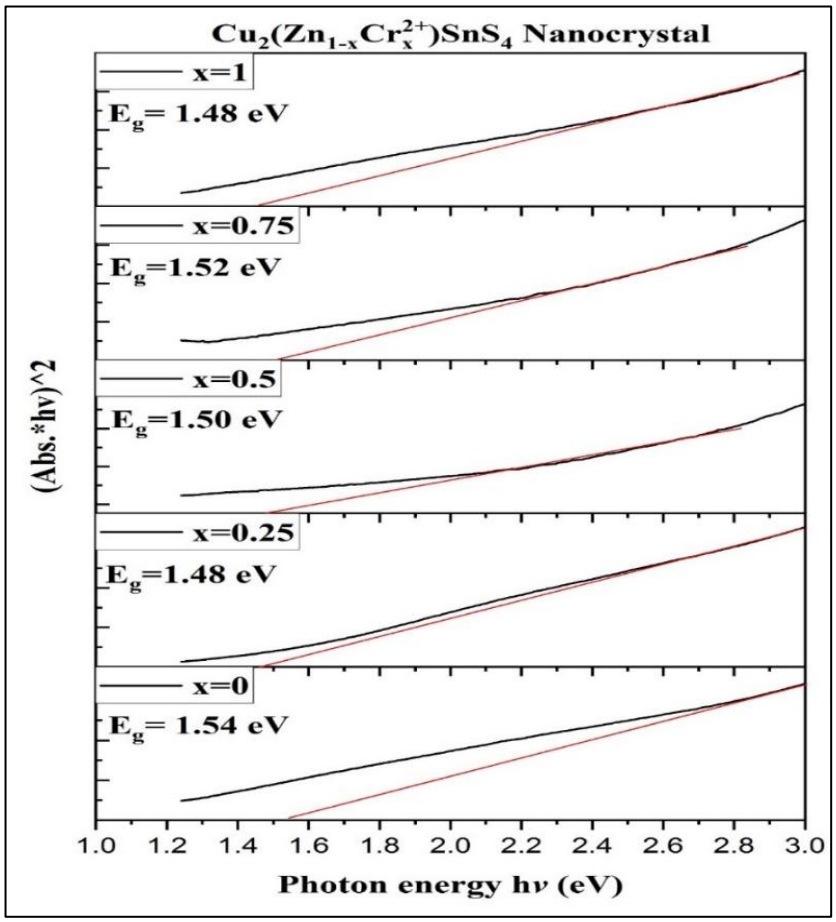

Fig. 4. Band gap energy of the $Cu_2Zn_{1-x}Cr_xSnS_4$ compound at (x = 0–1).

or structural modification did not result in rise to the emergence of an undesirable phase, but helped increase the regularity of crystal forged and reduce structural defects. This corresponds to FESEM results, shown to a homogeneous morphology and nanoparticles. Based on this, it can be concluded that the compound shows good structural stability, and supports goal applications such as photocatalysis or its ability to use in thin film solar cells.

Magnetic properties

The results of VSM measurement showed that pure Cu_2ZnSnS_4 compound at x = 0 shows no

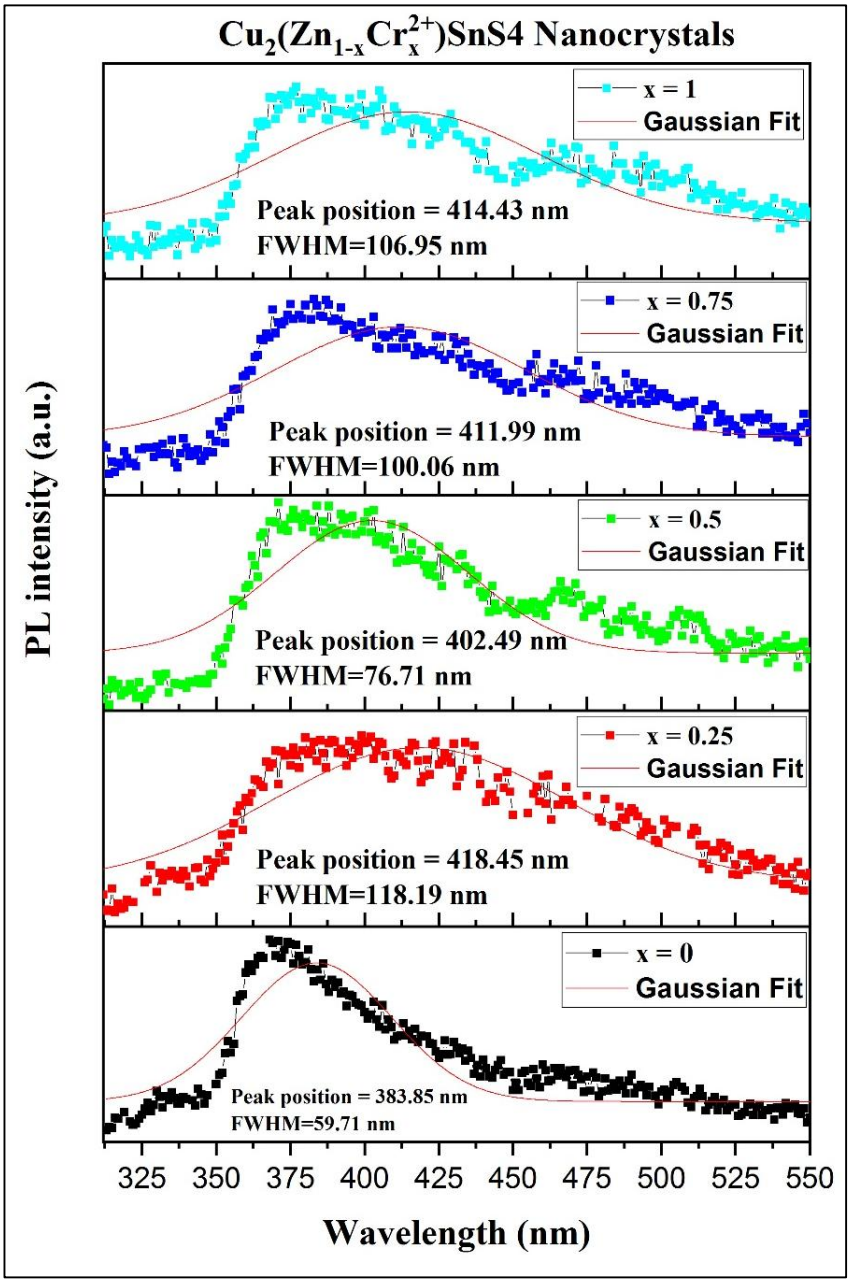

Fig. 5. Fluorescence spectrum of the $Cu_2Zn_{1-x}Cr_xSnS_4$ compound at (x = 0–1).

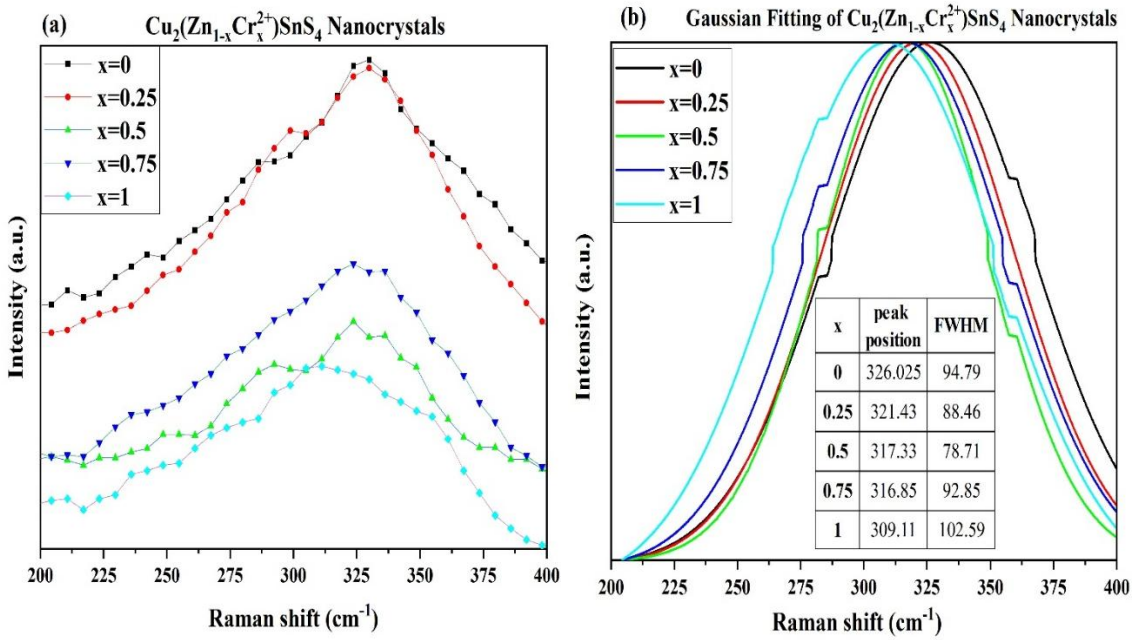

Fig. 6. Raman spectrum of the $Cu_2Zn_{1-x}Cr_xSnS_4$ compound at (x = 0–1).

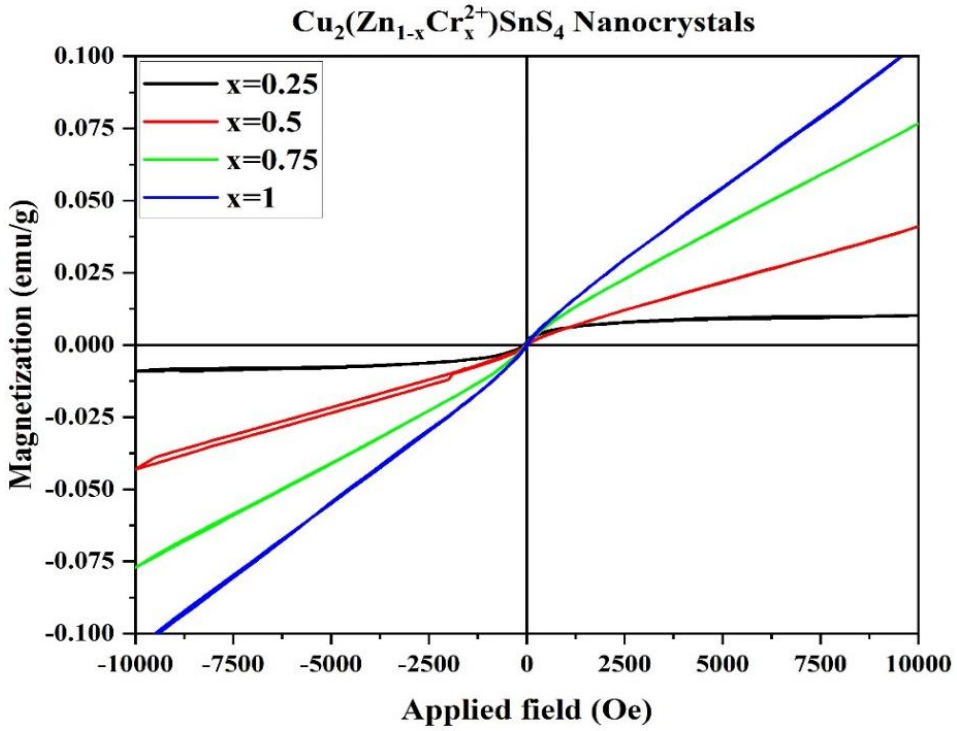

Fig. 7. Magnetization property of the $Cu_2Zn_{1-x}Cr_xSnS_4$ compound at (x = 0–1).

significant magnetic reaction, which corresponds to the non-magnetic nature of the Zn^{2+} ions. However, the Zn^{2+} ions gradually resulted in significant magnetic behavior with an increase in chrome content by changing the ions with Cr^{2+} ions. This shift can be explained by the fact that the Cr ions possess unpaired 3d electrons that contribute to the generation of local magnetic moments, in addition to the fact that the magnetic interactions between them occur via carrier-mediated exchange interactions, which enhances the overall magnetic property of the system [31]. XRD and Raman measurements also indicate the presence of cation disorder and an increase in structural defects with increasing Cr concentration, which contribute to enhancing the exchange pathways between Cr ions and thus strengthening the magnetic response [32]. In addition, the possibility of the formation of chromium-rich secondary phases (such as $ZnCr_2S_4$ or Cr–S clusters) with a strong magnetic nature cannot be ruled out, which may in turn contribute to an increase in the total magnetic moment, especially at high concentrations [33]. These results indicate that the Cu2ZnSnS4 compound can be converted from a non-magnetic semiconductor to a tunable, mildly magnetic semiconductor by introducing chromium, which improves the opto-magnetic properties. Absorption and fluorescence spectra revealed that replacing zinc ions with chromium ions narrows the optical bandgap and increases the density of defect states, which act as non-radiative recombination centers or additional emission centers, significantly affecting the intensity and shift of the emission peaks. Simultaneously, the defects themselves also contribute to the evolution of magnetic behavior by enhancing the magnetic bonding between chromium ions via charge carrier-mediated exchange interactions, leading to a gradual increase in magnetic moment with increasing chromium concentration, as illustrated in Fig. 7. This balance between optical and magnetic properties created by ionic substitution may pave the way for the use of these materials in multifunctional device applications such as spin-optics and magneto-optic energy conversion devices [34].

CONCLUSION

The ion substitution between zinc and chromium ions in the CZTS compound creates a series of complementary changes in physical properties. X-ray diffraction studies have shown that the crystal structure maintains its primary phase with a slight change in the lattice constants due to the difference in ionic radii between Zn^{2+} and Cr^{2+}, indicating the success of replacement without the formation of clear secondary phases. FESEM images have also shown that the morphology of nanoparticles remained relatively homogeneous with better grain distribution in specific concentrations, which directly affects the specific surface and reaction. Alternatively, UV-Visible absorption spectrum, calculation of energy gap and fluorescence spectra revealed that the introduction of chromium enclosure energy gap and increases the density of defect states, increases the light absorption efficiency of the visible region and represents a positive indication for photocatalytic. On the magnetic side, VSM measurements demonstrated that the pure CZTS compound is inherently non-magnetic, but it acquires increasing magnetic properties with increasing Cr concentration, due to the presence of unpaired 3d electrons and carrier-directed magnetic exchange mechanisms. Based on the structural, morphological, optical and magnetic properties that have been obtained, it is evident that ion substitution does not improve one property in isolation from the others, but rather promotes functional integration that makes this compound a strong candidate for advanced applications in thin film solar cells and photocatalysis.

ACKNOWLEDGEMENTS

The authors thank Al-Qasim Green University for providing laboratory support.

CONFLICT OF INTEREST

The authors declare that there is no conflict of interests regarding the publication of this manuscript.

REFERENCES

1. Shah UA, Wang A, Irfan Ullah M, Ishaq M, Shah IA, Zeng Y, et al. A Deep Dive into Cu_2ZnSn_4 (CZTS) Solar Cells: A Review of Exploring Roadblocks, Breakthroughs, and Shaping the Future. Small. 2024;20(30).
2. Hussein HM. Comparative Study between Spin Coated Cu_2ZnSn_4 and Cu_2FeSnS_4 Thin Films for Thin-Film Solar Cell Applications. Applied Solar Energy. 2022;58(6):751-759.
3. Hussein HM, Mohammed KA, Alsultany FH. Opto-Magnetic and Morphological Properties of the Quaternary CZCr+2TS Semiconductor. International Journal of Nanoscience. 2022;21(01).

4. Hussein EH, Hussein HM, Mohammed KA, Zbibah RS, Alrubaie AJ, Sharifi S, et al. Thermal and magnetic properties of chalcogenide CZFTS nanoparticles for solar cell application. Chalcogenide Letters. 2022;19(1):9-18.
5. Roy A, Sujatha Devi P, Karazhanov S, Mamedov D, Mallick TK, Sundaram S. A review on applications of Cu_2ZnSn_4 as alternative counter electrodes in dye-sensitized solar cells. AIP Advances. 2018;8(7).
6. Yang X, Qin X, Yan W, Zhang C, Zhang D, Guo B. Electronic Structure and Optical Properties of Cu_2ZnSn_4 under Stress Effect. Crystals. 2022;12(10):1454.
7. Sapeli MMI, Chelvanathan P, Yusoff Y, Rahman KS, Rafiq MKS, Shahahmadi SA, et al. Elucidating the effects of Cr–S variations in Cr-doped CZTS for intermediate band solar cell applications. Opt Mater. 2024;154:115790.
8. Praveenkumar N, Rao NM, Madhuri KV. Optical and magnetic properties of Cr-doped zinc phosphide nanoparticles prepared by the solid-state reaction method. Next Materials. 2025;8:100676.
9. Younus NC, Hussein HM. A competitive candidate for the Cu_2ZnSn_4 compound in solar photocatalytic degradation of organic pollutants. AIMS Materials Science. 2025;12(2):380-394.
10. Ajeel FN, AlGelal HMAA, Hamza LA, Ziadan KM, Al-Kabbi AS, Hussein HM, et al. I-V characteristic of tri ethanol amine capped CdSe thin films. AIP Conference Proceedings: AIP Publishing; 2023. p. 050015.
11. Ananthoju B, Mohapatra J, Jangid MK, Bahadur D, Medhekar NV, Aslam M. Cation/Anion Substitution in Cu_2ZnSn_4 for Improved Photovoltaic Performance. Sci Rep. 2016;6(1).
12. Shannon RD. Revised effective ionic radii and systematic studies of interatomic distances in halides and chalcogenides. Acta Crystallographica Section A. 1976;32(5):751-767.
13. Tablero C. Electronic and optical properties of substitutional V, Cr and Ir impurities in Cu_2ZnSn_4. Sol Energy Mater Sol Cells. 2014;125:8-13.
14. Mote VD, Purushotham Y, Dole BN. Williamson-Hall analysis in estimation of lattice strain in nanometer-sized ZnO particles. Journal of Theoretical and Applied Physics. 2012;6(1).
15. Himabindu B, Latha Devi NSMP, Rajini Kanth B. Microstructural parameters from X-ray peak profile analysis by Williamson-Hall models; A review. Materials Today: Proceedings. 2021;47:4891-4896.
16. Sapeli MMI, Ferdaous MT, Shahahmadi SA, Sopian K, Chelvanathan P, Amin N. Effects of Cr doping in the structural and optoelectronic properties of Cu_2ZnSn_4 (CZTS) thin film by magnetron co-sputtering. Mater Lett. 2018;221:22-25.
17. Mkawi EM. Kesterite Cu_2ZnSn_4 thin films synthesized utilizing electrodeposition: Influence of metal doping on the properties. International Journal of Energy Research. 2020;45(2):1908-1917.
18. Ma M, Sui Y, Zeng F, Zhao N, Wang T, Wang Z, et al. An efficient Cr-doping strategy to optimize the solution-processed Cu_2ZnSn_4 (S,Se)4 solar cells for better optoelectronic performance. J Alloys Compd. 2022;924:166476.
19. Khoshsirat N, Shafiei M, Wang H, Motta N. Investigation of the Doping Effect on Cu_2ZnSn_4 (CZTS) Thin Film Properties for Photovoltaic Applications. Proceedings of the International Conference on Advanced Light Absorbing Materials for Next Generation Photovoltaics; 2020/11/06: Fundació Scito; 2020.
20. Tobschall E. arXiv zieht um … und bleibt an der Cornell University. Front Matter; 2018. http://dx.doi.org/10.65527/5nwpw-jqv83
21. Sherka GT, Berry HD. Insight into impact of size and shape on optoelectronic properties of InX (X = As, Sb, and P) semiconductor nanoparticles: a theoretical study. Frontiers in Physics. 2024;12.
22. Larsen JK, Scragg JJS, Ross N, Platzer-Björkman C. Band Tails and Cu–Zn Disorder in Cu_2ZnSn_4 Solar Cells. ACS Applied Energy Materials. 2020;3(8):7520-7526.
23. Ananthoju B, Mohapatra J, Bahadur D, Medhekar NV, Aslam M. Influence of the Cu2ZnSnS4 nanoparticles size on solar cell performance. Sol Energy Mater Sol Cells. 2019;189:125-132.
24. Méndez-López A, Morales-Acevedo A, Acosta-Silva YJ, Ortega-López M. Synthesis and Characterization of Colloidal CZTS Nanocrystals by a Hot-Injection Method. Journal of Nanomaterials. 2016;2016:1-7.
25. Chelvanathan P, Shahahmadi SA, Ferdaous MT, Sapeli MMI, Sopian K, Amin N. Controllable formation of MoS2 via preferred crystallographic orientation modulation of DC-sputtered Mo thin film. Mater Lett. 2018;219:174-177.
26. Tiwari D, Yakushev MV, Koehler T, Cattelan M, Fox N, Martin RW, et al. Mapping the Energetics of Defect States in Cu_2ZnSn_4 films and the Impact of Sb Doping. ACS Applied Energy Materials. 2022;5(4):3933-3940.
27. Kaur K, Nisika, Chowdhury AH, Qiao Q, Kumar M. Nanoscale charge transport and local surface potential distribution to probe the defect passivation in Cr-substituted earth abundant CZTS absorber layer. J Alloys Compd. 2021;854:157160.
28. Wang Y, Ding Y, Ni J. Electronic structures of Fe-terminated armchair boron nitride nanoribbons. Appl Phys Lett. 2011;99(5).
29. Marshall MSJ, Kumah DP, Reiner JW, Baddorf AP, Ahn CH, Walker FJ. Piezoelectric force microscopy of crystalline oxide-semiconductor heterostructures. Appl Phys Lett. 2012;101(10):102902.
30. Siebentritt S. Why are kesterite solar cells not 20% efficient? Thin Solid Films. 2013;535:1-4.
31. Dietl T, Ohno H, Matsukura F, Cibert J, Ferrand D. Zener Model Description of Ferromagnetism in Zinc-Blende Magnetic Semiconductors. Science. 2000;287(5455):1019-1022.
32. Attarzadeh N, Kazemi A, Molaei M, Fattah-alhosseini A. Multipurpose surface modification of PEO coatings using tricalcium phosphate addition to improve the bedding for apatite compounds. J Alloys Compd. 2021;877:160275.
33. Lejda K, Drygaś M, Janik JF, Szczytko J, Twardowski A, Olejniczak Z. Magnetism of Kesterite Cu2ZnSnS4 Semiconductor Nanopowders Prepared by Mechanochemically Assisted Synthesis Method. Materials. 2020;13(16):3487.
34. Fattah-alhosseini A, Molaei M, Attarzadeh N, Babaei K, Attarzadeh F. On the enhanced antibacterial activity of plasma electrolytic oxidation (PEO) coatings that incorporate particles: A review. Ceram Int. 2020;46(13):20587-20607.